Dalton Transactions

Accepted Manuscript

This article can be cited before page numbers have been issued, to do this please use: X. Yu, S. Jiao, K. Li, W. Zhang, Y. Liu and Z. Huang, *Dalton Trans.*, 2014, DOI: 10.1039/C4DT03022B.

ROYAL SOCIETY OF CHEMISTRY

www.rsc.org/dalton

Dalton Transactions

Dynamic Article Links ►
View Article Online
DOI: 10.1039/C4DT03022B

Cite this: DOI: 10.1039/c0xx00000x

www.rsc.org/xxxxxx

ARTICLE TYPE

Cd(II)-Terpyridine-based complex as a ratiometric fluorescent probe for pyrophosphate detection in solution and as an imaging agent in living cells†

Shu-Yan Jiao, Kun Li*, Wei Zhang, Yan-Hong Liu, Zeng Huang and Xiao-Qi Yu*

Received (in XXX, XXX) Xth XXXXXXXXX 20XX, Accepted Xth XXXXXXXXX 20XX
DOI: 10.1039/b000000x

The terpyridine antracene ligand **L1** was synthesized and characterized. **L1** is a ratiometric fluorescent probe for Cd^{2+} with a recognition mechanism based on intramolecular charge transfer (ICT). An **L1-Cd(II)** complex was isolated, and its structure was established by single-crystal XRD. The **L1-Cd(II)** complex was able to serve as a novel reversible chemosensing ensemble to allow for ratiometric response to pyrophosphate (PPi) in aqueous media. Moreover, the fluorescence imaging in living cells from these two emission channels suggested that **L1** was a ratiometric probe for Cd^{2+}, and the in situ generated **L1-Cd(II)** complex was also a ratiometric ensemble for PPi detection in living cells.

Introduction

The recognition of phosphates represents an interesting and emerging field of research due to their crucial roles in a range of essential biological processes.[1] They have bioenergetic roles and are involved in genome stability, lipid stability, skeletal structure, protein regulation, cell signaling, the recognition of organelle membranes, and many other processes and events.[2] On the other hand, PPi (pyrophosphate $P_2O_7^{4-}$) is the product of ATP hydrolysis and an essential anion for normal cell function. For example, PPi is involved in energy transduction in organisms, and it controls metabolic processes through participation in various enzymatic reactions.[3,4] Additionally, an elevated PPi concentration in the synovial fluid is associated with calcium pyrophosphate dihydrate crystal deposition disease and a condition called chondrocalcinosis.[5] Therefore, it is necessary to develop methods that can detect PPi, especially methods with good selectivity.

Among various methodologies adopted for anion sensing in aqueous environments, metal ion-anion coordination has been recognized as one of the most popular for ions with high hydration energy, such as various phosphates.[6] Most often, among these sensors that contain metal complexes as the recognition units, Zn(II) complexes are frequently used,[7-9] but other metal ions such as Cu(II), Cd(II), Mn(II), Eu(III), and Tb(III)[10,11] have also been employed. The terpyridine derivatives, due to the suitably arranged ring nitrogens, have good abilities to coordinate with transition metals, because of their synthetic accessibility and excellent ability to bind with both low and high-oxidation state metal ions, many fluorescence reagents based on terpyridine derivatives have been reported for the detection of metal cations in solution, furthermore, these metal complexes of terpyridine derivatives could be extensively investigated for the fluorescent recognition of targets.[12]

Recently, Rissanen reported a simple fluorescent terpyridine-Zn(II) probe for PPi, which employs an "OFF-ON" process but wasn't a ratiometric probe for PPi.[13] Compared to intensity-based fluorescent sensors, ratiometric fluorescent sensors show an obvious advantage because they can eliminate most or all ambiguities by self-calibration through two emission bands. On the other hand, although many compounds have been reported as good sensors for PPi, only a limited number of systems can reversibly detect biophosphates.

In connection with our continuing research of fluorescent sensors for biologically and environmentally important ions, herein we reported a novel, reversible Cd(II)-terpyridine chemosensing ensemble that allows for ratiometric response to PPi. More importantly, this ensemble could be successfully used to recognize PPi in living cells.

Experimental

General

High Resolution Mass Spectrometer (HRMS) data were recorded on a Bruker Daltonics Bio TOF mass spectrometer, respectively. The ^{1}H NMR and ^{13}C NMR spectra measured on a Bruker AM400 NMR spectrometer and the δ scale in ppm referenced to residual solvent peaks or internal tetramethylsilane (TMS). Absorption spectra recorded on Hitachi U1900 spectrophotometer at 298 K. Fluorescence emission spectra were obtained using FluoroMax-4 Spectrofluorophotometer (HORIBA Jobin Yvon) at 298 K. The RAW264.7 cells were analyzed in an EICA TCS SP8 confocal laser microscopy. All of the solvents were either HPLC or spectroscopic grade in the optical spectroscopic studies.

Details for UV-vis and Fluorescence Measurements

Stock solutions of **L1** (1.0 mM) were prepared in absolute DMSO. The 0.01 M stock solutions of metal ions (Na^+, K^+, Mg^{2+}, Ca^{2+}, Mn^{2+}, Fe^{3+}, Co^{2+}, Ni^{2+}, Cu^{2+}, Ag^+, Zn^{2+}, Cd^{2+}, Pb^{2+} and Al^{3+})

View Article Online
DOI: 10.1039/C4DT03022B

were prepared in distilled water as their nitrate salts. Stock solutions of anions as sodium salts (F^-, Cl^-, Br^-, I^-, CH_3COO^-, SCN^-, SO_4^{2-}, CO_3^{2-}, NO_3^-, citrate, SO_3^{2-}, Pi, $C_2O_4^{2-}$, PPi) (0.01 M) and ATP, ADP (0.01 M) were prepared in distilled water.

Synthesis of Ligand L1

2-Acetylpyridine (0.61 g, 5.0 mmol) was added into a solution of 9-anthraldehyde (0.52 g, 2.5 mmol) in EtOH (25 mL), KOH pellets (0.39 g, 85%, 6.0 mmol) and aq NH_3 (7.5 mL, 30%, 6.3 mmol) were then added to the solution. The solution was heated at reflux for 24 h. After cooling down to ambient temperature, the solution was evaporated to dryness under reduced pressure to give the crude product, purification by a silica column afforded a yellow solid (0.24 g. 23%). Calcd for $C_{29}H_{20}N_3$ $[M+H^+]$, 410.1652, found 410.1647. ^1H NMR (400 MHz, $CDCl_3$) δ (ppm): 8.79(d, 2 H, *J* = 8.0 Hz), 8.63 (d, 2 H, *J* = 4.0 Hz), 8.61 (s, 2 H), 8.55(s, 1 H), 8.06 (d, 2 H, *J* = 8.0 Hz), 7.89(t, 2 H, *J* = 8.0 Hz), 7.71 (d, 2 H, *J* = 8.0 Hz), 7.46 (t, 2 H, *J* = 8.0 Hz), 7.32-7.37 (m, 4 H). ^{13}C NMR (100 MHz, $CDCl_3$), δ (ppm): 121.41, 123.82, 123.87, 125.84, 126.39, 127.35, 128.40, 129.54, 131.24, 134.33, 136.87, 149.23, 149.53, 155.71, 148.83, 156.18.

Synthesis of Ligand L1-Cd(II) complex

To a solution of **L1** (82 mg, 0.2 mmol) in CH_3CN (10 mL) was added $Cd(NO_3)_2 \cdot 4H_2O$ (61.6 mg, 0.2 mmol) and the resulting reaction mixture was reacted for 2 h at room temperature. After the solution was concentrated, a light yellow solid was obtained and dried in vacuo to give the desired product, **L1-Cd(II)** complex (yield 93%). ^1H NMR (400 MHz, CD_3OD) δ (ppm): 8.95(d, 4 H, *J* = 4.0 Hz), 8.85 (s, 4 H), 8.78 (s, 2 H), 8.65(d, 4 H *J* = 8.0 Hz), 8.20-8.26 (m, 8 H), 7.85-7.88 (m, 4 H), 7.66 (d, 4 H *J* = 8.0 Hz), 7.54-7.58 (m, 4 H), 7.47-7.49 (m, 4 H). ^{13}C NMR (100 MHz, CD_3OD), δ (ppm): 124.73, 126.17, 126.70, 127.32, 128.05, 128.38, 129.92, 130.01, 130.72, 132.79, 133.01, 142.27, 150.23, 151.23, 151.44, 156.29. Crystal data for **L1-Cd(II)** complex: empirical formula: $C_{58}H_{38}Cd_2N_{10}O_{12}$; formula weight: 1291.78; temperature: 293 K; radiation Cu Kα; crystal system: triclinic P-1; unit cell dimensions: a= 9.3678(5), b=11.1675(6), c=13.9177(7); α=70.867(5), β =83.835(4), γ=69.788(5); V=1290.83 $Å^3$; Z=1; Dcalc=1.662 g/cm^3; F(000)= 648.0; 2θ range: 8.88 Å-117.854 Å; Final R indices [I>2σ(I)]: R1=0.0446, wR2=0.1135; Final R indices [all data]: R1=0.0461, wR2=0.1155; Crystal size (mm^3): 0.6×0.5×0.3;

Cellular Imaging Methodology

RAW 264.7 cells were cultured in Dulbecco's Modified Eagle's Medium (DMEM) supplemented with 10% fetal bovine serum, 2.2 g/L sodium bicarbonate, and 1% antibiotic-antimycotic solution containing streptomycin and penicillin. Cells were maintained under a humidified atmosphere of 5% CO_2 and 95% air in a 37 °C incubator. Stock solution (1 mM) of the conjugate of **L1** was prepared in DMSO. RAW 264.7 cells were seeded at a density of 5×10^5 cells /mL in glass-bottom cell culture dishes. After 24 h of seeding, DMEM media was removed and dishes were washed twice carefully with HEPES. Cells were incubated in the presence of 10 μM **L1** for 30 min. Then the PBS containing some traces of ligand was removed and dishes were washed three times with PBS. At this stage, cells were imaged for intrinsic fluorescence of **L1** using EICA TCS SP8 confocal laser microscopy, further, the cells were incubated with 20 μM Cd^{2+} diluted in PBS for 30 min, After the incubation, the PBS containing Cd^{2+} was removed and the cells were washed three times with PBS, subsequently cells were imaged by EICA TCS SP8 confocal laser microscopy, finally, the above cells were incubated with 40 μM PPi, cells were imaged by EICA TCS SP8 confocal laser microscopy as well. The exposure time was kept the same for all the cases.

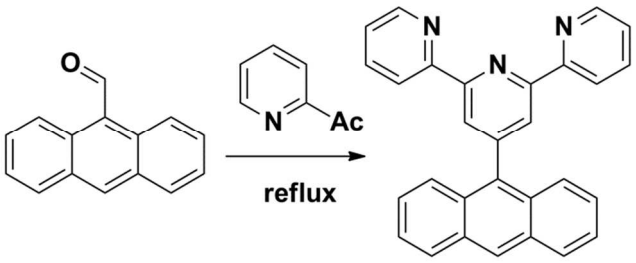

Scheme 1 Synthesis route for the Ligand **L1**

Results and discuSssion

L1 was synthesized from 9-anthraldehyde by the addition of 2-Acetylpyridine, KOH and $NH_3 \cdot H_2O$ in EtOH under reflux (Scheme 1). Detailed synthetic procedures and characterization data are provided in the Experimental Section. The **L1-Cd(II)** conjugate has been obtained in quantitative yield by reacting **L1** with $Cd(NO_3)_2 \cdot 4H_2O$ in CH_3CN as detailed in the Experimental Section. **L1** and the **L1-Cd(II)** complex were characterized by various analytical and spectral techniques. The molecular structure of **L1-Cd(II)** complex was established on the basis of single-crystal XRD data.

Cation Recognition Studies

The binding, recognition, and selectivity of **L1** toward metal ions, including Cd^{2+}, Zn^{2+}, Li^+, Na^+, K^+, Ca^{2+}, Ag^+, Al^{3+}, Fe^{3+}, Ni^{2+}, Cu^{2+}, Co^{2+}, and Mn^{2+}, were investigated. As shown in Fig. 1 and Fig.S1, **L1** has strong fluorescence emission at 421 nm, and there was a new emission peak at 553 nm upon the addition of Zn^{2+} or Cd^{2+}, that did not respond to Li^+, Na^+, K^+, or Ca^{2+}. In addition, a moderate decrease of the emission intensity of **L1** was observed in the presence of Ag^+, Al^{3+}, Fe^{3+}, Ni^{2+}, and the emission intensity of **L1** was absolutely quenched by Cu^{2+}, Co^{2+}, and Mn^{2+} (Fig.S1).Therefore, **L1** was only a ratiometric fluorescent sensor for Cd^{2+} and Zn^{2+}. In general, there are two types of fluorescent sensors suitable for ratiometric investigations. One type is based on fluorescence resonance energy transfer, which requires the chemical conjugation of two different fluorophores, the other is based on the intramolecualr charge transfer (ICT) mechanism which is more widely utilized in ionic sensing, molecular switching, and fluorescent labeling.[14] The red shift of the fluorescent emission of **L1** after coordination with Cd(II) can be ascribed to the electron-donating ability of the anthracene group, which caused intramolecular charge transfer (ICT) from the anthracene to the Cd(II)-coordinated terpyridine. Moreover, **L1** can selectively respond to Cd^{2+} over Zn^{2+}; upon the addition of Cd^{2+}, the ratio of the emission intensities at 553 nm and 421 nm increased from 0.018 to 30, whereas upon the addition of Zn^{2+}, this ratio only increased from 0.018 to 9.7. The ratios in the presence of all other metal ions were calculated and displayed no significant changes (Fig. 2).

View Article Online
DOI: 10.1039/C4DT03022B

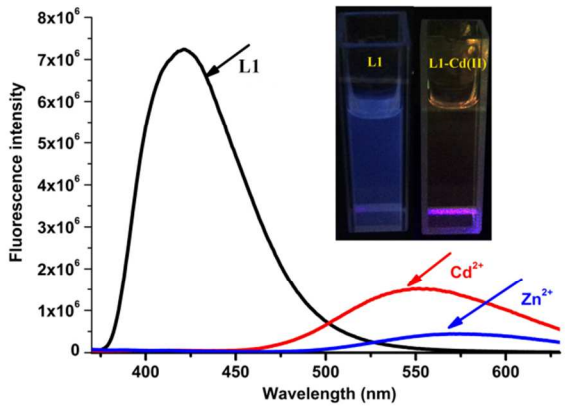

Fig. 1 Emission spectra of **L1** (10 μM) with Zn^{2+} and Cd^{2+} (50 μM) in CH_3CN, λex=326 nm. Inset: visual change in fluorescence of **L1** in the presence of Cd^{2+}

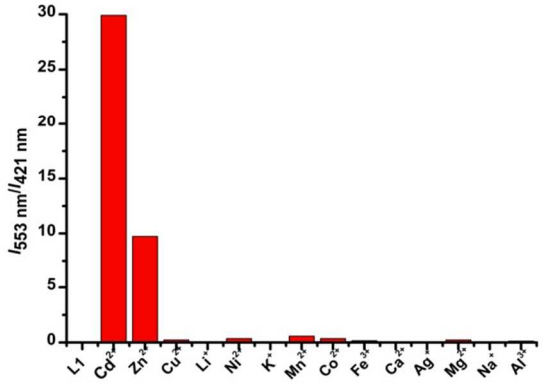

Fig. 2 Emission ratio ($I_{553\ nm}/I_{421\ nm}$) of **L1** (10 μM) in the presence of various metal ions (50 μM) in CH_3CN, λex=326 nm.

Accordingly, upon excitation at 326 nm, the emission at 421 nm decreased, and a new emission peak at 553 nm appeared, which gradually increased in intensity with increased Cd^{2+} concentration. The changes in the fluorescence spectrum stopped when the amount of added Cd^{2+} reached 1.0 equivalent of probe. At this amount, the ratio of the emission intensities at 553 nm and 421 nm ($I_{553\ nm}/I_{421\ nm}$) reached 30 times of the ratio in the absence of Cd^{2+}. The color of the fluorescence clearly changed from blue to light yellow. A well-defined isoemission point at 500 nm was also observed. Fluorescence titration experiments for **L1** with different concentrations of Cd^{2+} indicated the formation of an **L1-Cd(II)** complex (Fig. 3). The 2:2 binding stoichiometry of **L1** and Cd^{2+} was verified by a single-crystal structure (Fig. 4) and mass spectrometry (HRMS) (Fig.S2). The peak at 1232.1163 corresponds to a 2:2 complex formation [$2L1+2Cd(NO_3)_2$-NO_3^-].The UV-vis absorption spectra of **L1** in the presence of various concentrations of Cd^{2+} were also studied. When the Cd^{2+} was gradually added, the maximum absorption at 325 nm increased gradually. Meanwhile, the absorption at 365 nm and 385 nm was nearly unchanged (Fig. S3).These results further validated complex formation between **L1** and Cd^{2+}.

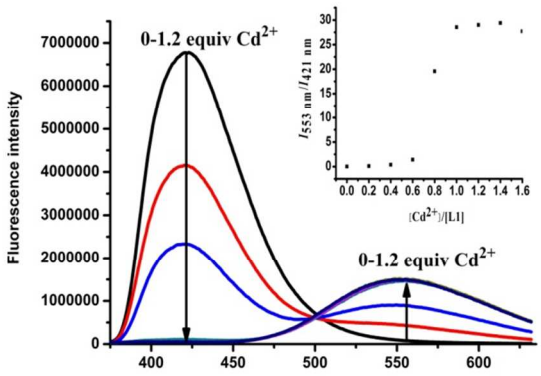

Fig. 3 Fluorescence emission spectra of L1 upon the addition of Cd^{2+} in CH_3CN, [L1]=[10 μM], [Cd^{2+}]=[0 μM, 1 μM, 2 μM, 3 μM, 4 μM, 5 μM, 6 μM, 7 μM, 8 μM, 9 μM, 10 μM, 11 μM, and 12 μM]. Inset: plot of emission ratio ($I_{553\ nm}/I_{421\ nm}$) versus [Cd^{2+}].

Single-crystal XRD structure of L1-Cd(II) complex.

Single crystal of **L1-Cd(II)** suitable for X-ray diffraction were grown from a CH_3OH / CH_2Cl_2 / hexane solvent mixture. There was no solvent of crystallization. This complex crystallizes in the triclinic system with space group P-1. The details of the data collection and the structure refinement are given in the Experimental Section. Single-crystal x-ray diffraction analysis revealed that the crystal structure of the **L1-Cd(II)** complex is a 2:2 dimer ([L-$Cd(NO_3)_2$]$_2$) possessing a center of symmetry. Each Cd(II) atom is coordinated to three chelating nitrogen atoms from terpyridine and five oxygen atoms from nitrates. Its structure also reveals that both Cd(II) centers adopt a distorted bicapped trigonal-priamatic geometry (Fig.5a), the N atoms trapped in Fig.5a by red ellipsoid were the tops of caps in the distorted bicapped trigonal-priamatic geometry. The dimeric complex is formed by the coupling of [L1-$Cd(NO_3)_2$] units linked by two oxygen atoms and two Cd(II) atoms. The two oxygen atoms and two Cd(II) atoms form a parallelogram, and these four atoms are in the same plane. The two Cd(II) centers are 4.220Å apart. The distance from O_2–O_2[1] is 2.926 Å. The other important bond distances and dihedral angles of the **L1-Cd(II)** complex are listed in Table 1. In addition, in this structure, we found that the two terpyridines are parallel, and the vertical distance of the two terpyridines is approximate 2.535 Å. The anthracene groups are also parallel. The vertical distance of the two anthracene groups is approximately 15.605 Å. Moreover, in the lattice formed by the dimer **L1-Cd(II)** complex (Fig. 5b), π-π stacking of terpyridines and anthracene groups was observed and may result in the quenching of fluorescence. This result is consistent with the fluorescence properties that were mentioned in Fig. 1, where the addition of Cd^{2+} to the **L1** solution gradually decreased the fluorescence intensity at 421 nm.

View Article Online
DOI: 10.1039/C4DT03022B

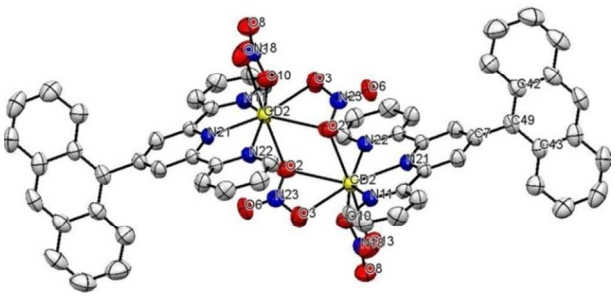

Fig. 4 X-ray crystal structure of **L1-Cd(II)** complex. All the hydrogen atoms are omitted for clarity.

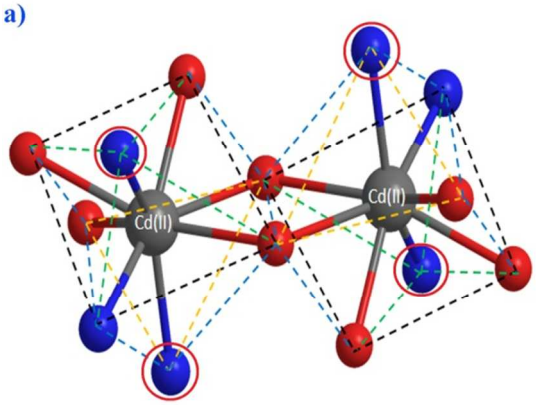

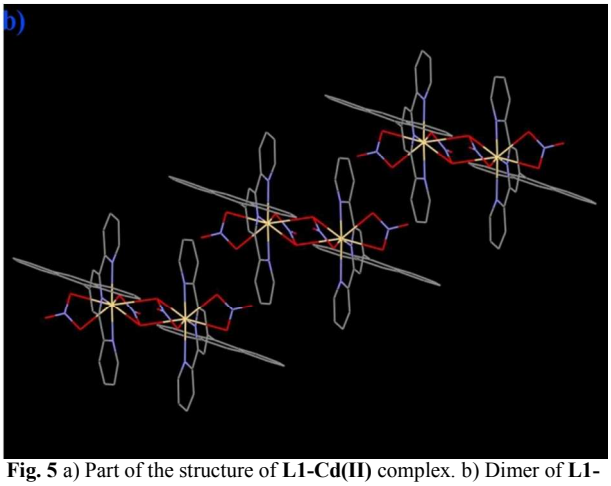

Fig. 5 a) Part of the structure of **L1-Cd(II)** complex. b) Dimer of **L1-Cd(II)** complex formed in the lattice.

Fluorescence Titration of L1-Cd(II) complex with anions

The recognition behavior of the **L1-Cd(II)** complex 10 μM was evaluated by performing fluorescence titrations in 1:1 HEPES/CH_3CN with different anions, including 50 μM PPi, F^-, SCN^-, CO_3^{2-}, Br^-, PO_4^{3-}, NO_3^-, AcO^-, citrate, I^-, N_3^-, SO_4^{2-}, $C_2O_4^{2-}$, SO_3^{2-}, and Cl^-, and with the nucleotides ATP and ADP. As shown in Fig. 6, all the anion titrations except PPi and ATP caused almost no significant changes in the fluorescence. When PPi or ATP was added, the fluorescence intensity of the **L1-Cd(II)** complex at 560 nm decreased gradually, and an emission peak at 431 nm appeared; thus, the **L1-Cd(II)** complex shows ratiometric response to PPi (Fig.6) and ATP (Fig.6 inset). Furthermore, **L1-Cd(II)** can selectively respond to PPi compared to ATP (Fig. 7); upon the addition of PPi to **L1-Cd(II)** in solution, the ratio of the emission intensities at 560 nm and 431 nm increased from 0.26 to 7.46, whereas the addition of ATP only increased this ratio from 0.26 to 2.66. In addition, upon addition of PPi to **L1-Cd(II)** in solution, the fluorescence intensity and emission wavelength were the same to **L1**. The results suggested that only PPi could completely de-complex the **L1-Cd(II)** complex.

Table 1. Important Bond Distance and Dihedral Angles of **L1-Cd(II)** complex

L1-Cd(II) complex	angle (°)/ distance (Å)
C42-C49-C7/Cd2-N21	119.4(4)/ 2.311(3)
C43-C49-C7/Cd2-N22	119.5(4)/ 2.359(3)
C1-N21-Cd2/Cd2-N11	119.8(3)/ 2.363(3)
N21-Cd2-N22/Cd2-O10	69.45(11)/ 2.462(4)
N21-Cd2-N11/Cd2-O13	70.05(11)/ 2.504(4)
O21-Cd2-O31/Cd2-O2	51.92(11)/ 2.591(3)
O21-Cd2-O21/Cd2-O21	69.48(13)/ 2.544
Cd2-O2-Cd21/ Cd2-O31	110.52(13)/ 2.352
O10-Cd2-O13/C49-C7	149.37(12)/ 1.499(6)
O2-N23-O6	123.3(4)
O3-N23-O2	116.4(4)
O3-N23-O6	120.3(4)

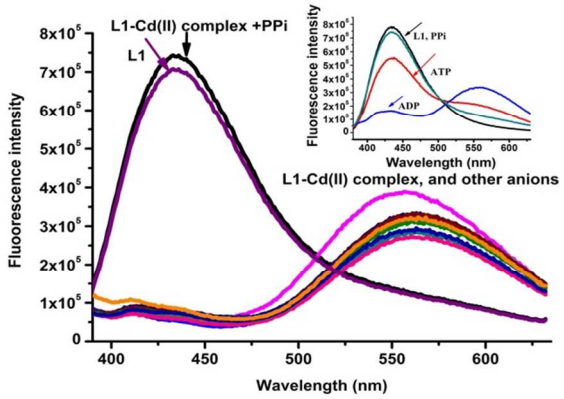

Fig.6 Emission spectra of **L1-Cd(II)** (10 μM) with various anions viz. PPi, F^-, SCN^-, CO_3^{2-}, Br^-, PO_4^{3-}, NO_3^-, AcO^-, Citrate, I^-, N_3^-, SO_4^{2-}, $C_2O_4^{2-}$, SO_3^{2-}, ClO_4^- (50 μM) in CH_3CN/HEPES (10 mM, pH=7.4) =1:1(v:v,), λex=326 nm. Inset: Emission spectra of **L1-Cd(II)** complex (10 μM) and **L1-Cd(II)** complex with PPi, ATP, ADP.

We found that the addition of trace amounts of PPi (0.5 μM, Fig.8) causes the fluorescence signal to change rapidly, which is very important for real-time detection. Therefore, the following titration experiments were carried out after addition of PPi. Accordingly, upon excitation at 326 nm, the emission at 560 nm

View Article Online
DOI: 10.1039/C4DT03022B

decreased and an emission at 431 nm appeared, which gradually increased in intensity with increased PPi concentrations. These changes in the fluorescence spectrum stopped when the amount of added PPi reached 1.3 equivalent of **L1-Cd(II)** complex, (Fig.8). Moreover, the detection limit for PPi was estimated to be 3.39 μM (Fig.S4). The proposed sensing mechanism of **L1-Cd(II)** complex towards PPi was illustrated in Scheme.2. An equilibrium competition constant, Kcomp was calculated on the basis of the titration data. The data are fit to a displacement model that provides an equilibrium competition constant (Kcomp $=5.44 \times 10^4 M^{-1}$, R=0.99498) in CH_3CN/HEPES=1:1(v:v) at pH=7.4 (Fig.9)[15]. This suggested that the binding affinity between PPi and Cd^{2+} was much more potent than that between **L1** and Cd^{2+}, and Cd^{2+} could be removed from the complex **L1-Cd(II)** complex by PPi. To further look into the nature of the interaction between **L1-Cd(II)** complex and PPi, HRMS experiments were carried out (Fig.S5). When 1 equiv of PPi was added to this complex, the peak at m/z1232.1163 corresponding to [2L1-2Cd(II)-$3NO_3^-$] disappeared and only the peak at m/z 410.1653 corresponding to [L1+H^+] was observed. This also indicated that PPi could remove Cd^{2+} from the complex **L1-Cd(II)** and then free **L1** was released from **L1-Cd(II)**.

The UV-vis absorption of **L1-Cd(II)** complex towards PPi in CH_3CN/HEPES=1:1 were investigated. As shown in Fig.S6, when added PPi into **L1-Cd(II)** complex in solution, the spectra was similar to **L1**, the results demonstrated that **L1-Cd(II)** complex could serve as an ensemble for selectively sense of PPi via a displacement mode.

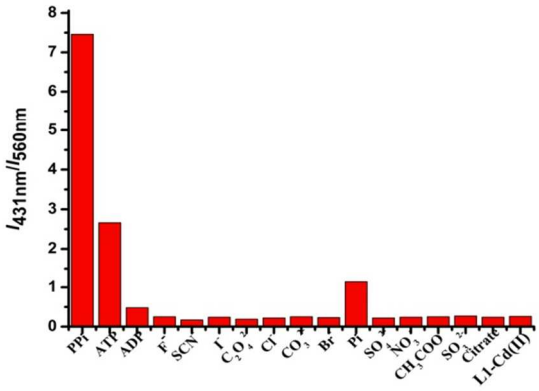

Fig.7 Ratio of emissions ($I_{431\,nm}/I_{560\,nm}$) of **L1-Cd(II)** complex to various anions in CH_3CN/HEPES(10 mM, pH=7.4)=1:1(v:v), λex=326 nm.

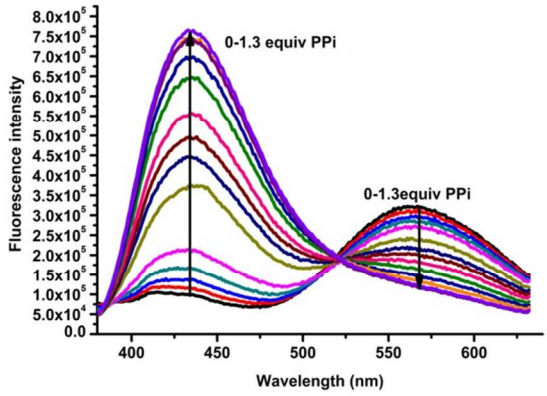

Fig.8 Fluorescence emission spectra of **L1–Cd(II)** upon addition of PPi in CH_3CN/HEPES(10 mM, pH=7.4)=1:1(v:v), [**L1-Cd(II)**]=[10 μM], [PPi]=[0μM, 5 μM, 1μM, 2 μM, 3 μM, 4 μM, 5 μM, 6 μM, 7 μM, 8 μM, 9 μM, 10 μM, 11 μM, 12 μM, 13 μM].

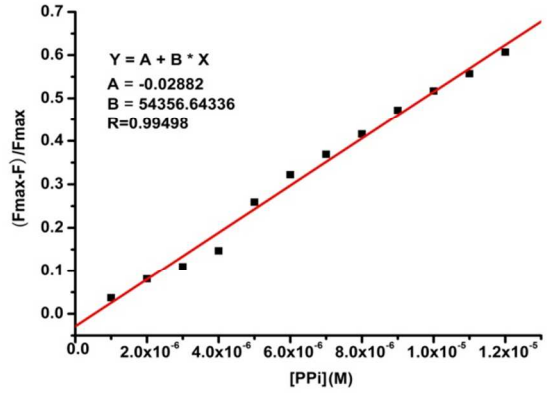

Fig.9 Fitting of competitive titrations of aqueous solutions containing chemosensing ensembles (**L1-Cd(II)**, 10 μM) with PPi in CH_3CN/HEPES(10 mM, pH=7.4) =1:1(v:v). λem =560 nm, λex=326 nm.

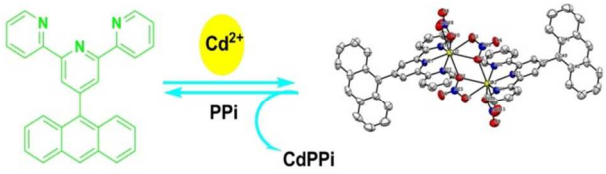

Scheme.2 Proposed Sensing Mechanism of **L1-Cd(II)** complex towards PPi.

We further carried out the competitive experiments using solution containing PPi and all other anions. Fig.10 indicates that the PPi-dependent fluorescence change of the complex **L1-Cd(II)** was not affected by the presence of the other anions. The results of competitive experiments suggest that the **L1-Cd(II)** complex shows good selectivity for PPi among other tested anions.

View Article Online
DOI: 10.1039/C4DT03022B

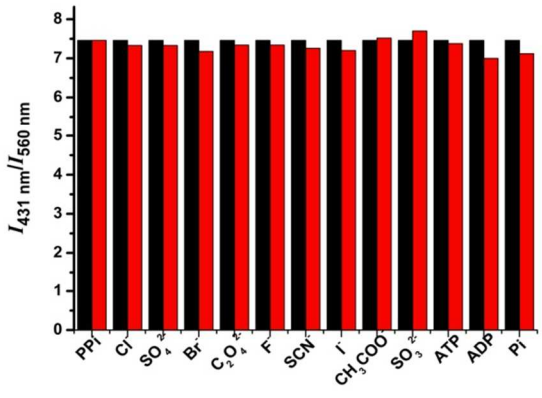

Fig.10 Ratio of emissions ($I_{431\ nm}/I_{560\ nm}$) in situ prepared **L1-Cd(Ⅱ)** complex (10 μM) with 5 equiv various anions in the absence and presence of PPi (10 μM) CH_3CN/HEPES (10 mM, pH=7.4) =1:1(v:v), λex=326 nm.

Reusability and Reversibility of Ligand L1

The reversible sensing behavior of **L1** was investigated by emission spectroscopy over five cycles by the addition of Cd^{2+} followed by PPi, a blue shift of the fluorescence emission peak of **L1-Cd(II)** complex from 560 nm to 431 nm upon addition of PPi through the formation of Cd-PPi complex, which releases the free **L1**. The free ligand **L1** is now able to bind Cd^{2+} and thereafter form the **L1-Cd(II)** complex which has a large fluorescence emission at 560 nm. This behavior of red and blue shift in fluorescence emission was monitored by addition of Cd^{2+} followed by addition of PPi over five successive cycles. Notable reversal of the shift in the fluorescence emission and fluorescence color change was observed in those five cycles (Fig.11 a,b). These findings strongly suggested that **L1** is a reversible and recyclable sensor for Cd^{2+} and its cadmium complex is a sencondary sensor for PPi.

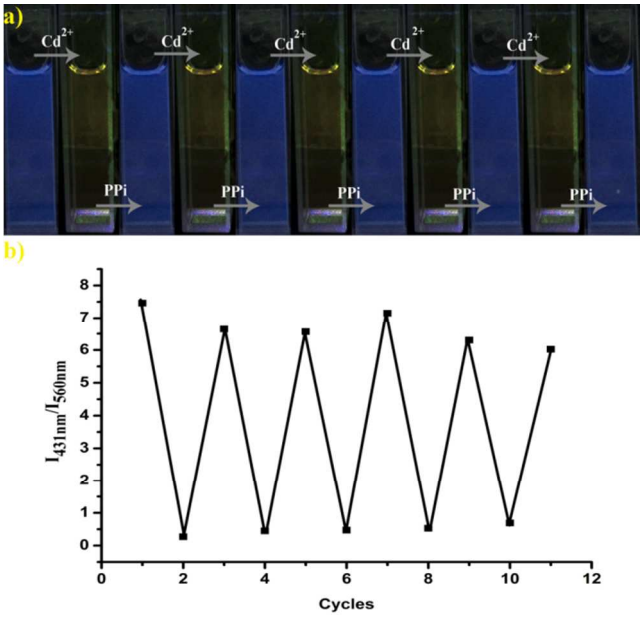

Fig.11 a) visual fluorescent color changes after each addition of Cd^{2+} and PPi sequentially: 1=**L1**; 2=[A+Cd^{2+}]; 3=[B+PPi]; 4=[C+Cd^{2+}]; 5=[D+PPi]; 6=[E+Cd^{2+}]; 7=[F+PPi]; 8=[G+Cd^{2+}]; 9=[H+PPi]; 10=[I+Cd^{2+}]; 11=[J+PPi]. b) Reversible and recyclable behavior of **L1** upon the sequential addition of Cd^{2+} followed by PPi in the fluorescence experiment observing the changes in the ratio intensity of emissions ($I_{431\ nm}/I_{560\ nm}$).

Confocal Fluorescence Imaging of L1-Cd(II) with PPi in living cells through two emission channels

Finally, due to the good chemical and spectroscopic properties of the probe, **L1** was applied for confocal fluorescence imaging in living RAW264.7 cells. As shown from Fig.12, RAW264.7 cells were incubated with **L1** (10 μM) for 0.5 h showed strong blue fluorescence at 420 nm-460 nm (Fig.12b) while the green fluorescence image obtained at 530 nm-570 nm was very weak(Fig.12c). By contrast, after the addition of Cd^{2+} and then incubation for another 0.5h, the fluorescence intensity in the green channel increased obviously (Fig.12e) and the blue fluorescence became weakly simultaneously (Fig.12f). However, when **L1** and Cd^{2+} pre-incubated RAW264.7 cells were further treated with PPi for 0.5 h, the blue fluorescence intensity in the blue channel increased obviously (Fig.12h) and the green fluorescence became very weak (Fig.12i) The cellular studies clearly indicate that **L1** exhibits good cell permeability and could be used to image Cd^{2+} in living cells. Moreover, the results also suggest that **L1-Cd(II)** complex can allow the ratiometric visualization of PPi in living cells.

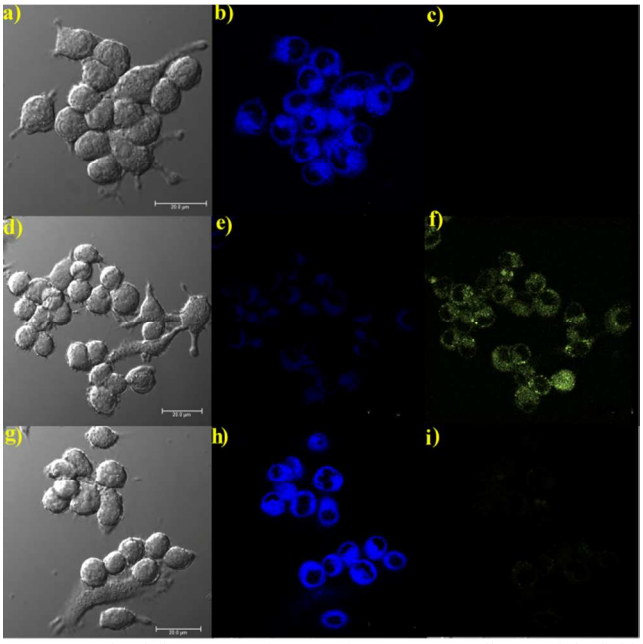

Fig.12 Confocal fluorescence images of RAW 264.7 cells. a) Bright field image when treated with **L1**(10 μM); (b) Blue-channel fluorescence image of a) detected at 420 nm-460 nm; c) Green-channel fluorescence image of a) detected at 530 nm-570 nm; d) Bright field image when treated with **L1**(10 μM) followed by 20 μM Cd^{2+}; e) Blue-channel fluorescence image of d) detected at 420 nm-460 nm; f) Green-channel fluorescence image of d) detected at 530 nm-570 nm; g) Bright images when treated with **L1-Cd(II)** complex followed by 20 μM PPi; h) Blue-channel fluorescence image of g) detected at 420nm-460nm; i) Green-channel fluorescence image of g) detected at 530 nm-570 nm;

Conclusions

Terpyridine linked anthracene conjugate **L1** was synthesized and characterized. It was found to be a ratiometric fluorescence probe for Cd^{2+}. The interaction of **L1** and Cd^{2+} were demonstrated on the basis of fluorescence, HRMS, visual

View Article Online
DOI: 10.1039/C4DT03022B

fluorescent color change and the recognition mechanism of **L1** for Cd^{2+} is based on intramolecular charge transfer (ICT) process. Moreover, the single-crystal XRD structure of **L1-Cd(II)** complex demonstrated **L1** and Cd^{2+} formed 2:2 dimer, viz., $[L\text{-}Cd(NO_3)_2]_2$. Each Cd(II) atom is coordinated to three chelating nitrogen atoms from terpyridyl and five oxygen atoms from nitrates. Its structure also reveals that both Cd(II) centers a distorted bicapped trigonal priamatical geometry, and the dimeric complex is formed by couples of $[L1\text{-}Cd(NO_3)_2]$ units linked by two oxygen atoms and two Cd(II) atoms. Besides, a novel reversible **L1-Cd(II)** chemosensing ensemble which allows for ratiometric response to PPi via a displacement mode. In accession, the fluorescence imaging from two emission channels in living cells suggest that **L1** successfully showed ratiometric respond to Cd^{2+} in living cells and the in situ **L1-Cd(II)** complex was a ratiometric sensor for PPi in living cells as well.

Acknowledgements

This work was financially supported by the National Program on Key Basic Research Project of China (973 Program, 2012CB720603 and 2013CB328900), the National Science Foundation of China (Nos. 21232005, 21472131, J1310008 and J1103315). and the Specialized Research Fund for the Doctoral Program of Higher Education in China (20120181130006). We also thank the Analytical & Testing Center of Sichuan University for NMR analysis.

Notes and references

Key Laboratory of Green Chemistry and Technology, Ministry of Education, College of Chemistry, Sichuan University, Chengdu, 610064, China Fax: (86)-28-85415886 ; Tel: (86)-28-85415886; E-mail: kli@scu.edu.cn; xqyu@scu.edu.cn

Electronic Supplementary Information (ESI) available: [NMR and HRMS spectras]. See DOI: 10.1039/b000000x/

1 a) S. K. Kim, D. H. Lee, J. N. Hong and J. Yoon, *Acc. Chem. Res.,* 2009, **42,** 23; b) G. V. Zyryanov, M. A. Palacios and P. Anzenbacher, *Angew. Chem., Int. Ed.,* 2007, **46,** 1; c) R. K. Pathak, V. K. Hinge, A. Rai, D. Panda and C. P. Rao, *Inorg. Chem.* 2012, **51,** 4994.

2 a) O. G. Tsay, S. J. Manjare, H. Kim, K. M. Lee, Y. S. Lee and D. G. Churchill, *Inorg. Chem.* 2013, **52,** 10052; b) A. K. H. Hirsch, F. R. Fischer and F. Diederich, *Angew. Chem., Int. Ed.,* 2007, **46,** 338; c) M. W. Bowler, M. J. Chiff, J. P. Waltho, G. M. Blackbum, *New J. Chem.* 2010, **34,** 784.

3 a) J. H. Wen, Z. R. Geng, Y. X. Yin, Z. Zhang and Z. L. Wang, *Dalton Trans.,* 2011, **40,** 1984; b) R. Joseph, J. P. Chinta and C. P. Rao, *Inorg. Chem.,* 2011, **50,** 7050; c) W. Saenger, *Principles of Nucleic Acid Structure;* Springer: New York, **1998**; d) W. H. Chen, Y. Xing and Y. Pang, *Org. Lett.* 2011, **13,** 1362.

4 a) J. H. Lee, A. R. Jeong, J. H. Jung, C. M. Park and J. I. Hong, *J. Org. Chem.,* 2011, **76,** 417; b) P. Nyŕen, *Anal. Biochem.,* 1987, **167,** 235; c) M. Ronaghi, S. Karamohamed, B. Pettersson, M. Uhlen and P. Nyŕen, *Anal.* Biochem., 1996, **242,** 84; d) T. Tabary, L. Ju, *J. Immumol. Meth.,* 1992, **156,** 55.

5 a) A. S. Rao, S. Singha, W. Y. Choi and K. H. Ahn, *Org. Biomol. Chem.,* 2012, **10,** 8410; b) M. Doherty, C. Becher, M. Regan, A. Jones, J. Ledingham, *Ann, Rheum. Dis.,* 1996, **66,** 432; c) A. E. Timms, Y. Zhang, R. G. Russell, M. A. Brown, *Rheumatology,* 2002, **41,** 725; d) S. Nussey, S. Whitehead, *Endocrinology: An Integrated Approach; BIOS Scientific Publishers: Oxford, U.K.,* 2001; e) J. H. Lee, J. Park, M. S. Lah, J. Chin, J. I. Hong, *Org. Lett.,* 2007**, 9,** 3729.

6 a) J. Gao, T. Riss-Johannessen, R. Scopelliti, X. H. Qian, K. Severin, *Dalton Trans.,* 2010, **39***,* 7114; b) X. J. Zhao, L. He, C. Z. Huang, *Talanta,* 2012, **101***,* 59; c) H. W. Rhee, H. Y. Choi, K. Han and J. I. Hong, *J. Am. Chem. Soc.,* 2007, **129,** 4524.

7 a) C. Park and J. I. Hong, *Tetrohedron Lett.,* 2010, **51,** 1960; b) X. H. Huang, Y. Lu, Y. B. He, Z. H. Chen, *Eur. J. Org. Chem.,* 2010, 1921; c) S. Khatua, S. H. Choi, J. Lee, K. Kim, Y. Do and D. G. Churchill, *Inorg. Chem.,* 2009, **48,** 2993; d) M. K. Coggins, A. M. Parker, A. Mangalum, G. A. Galdamez and R.C. Smith, *Eur. J. Org. Chem.,* 2009, 343.

8 a) L. Tang, Y. Li, H. Zhang, Z. Guo and J. Qian, *Tetrohedron Lett.,* 2009, **50,** 6844; b) G. Su, Z. Liu, Z. Xie, F. Qian, W. He and Z. Guo, *Dalton Trans.,* 2009, 7888; c) G. Ambrosi, M. Formica, V. Fusi, L. Giorgi, A. Guerri, E. Macedi, M. Micheloni, P. Paoli, R. Pontllini and P. Rossi, *Inorg. Chem.,* 2009, **48,** 5901; d) J. V. Carolan, S. J. Butler, K. A. Jolliffe, *J. Org. Chem.,* 2009, **74,** 2992.

9 a) L. Rodríguez, J. G. Lima, A. J. Parola, F. Pina, R. Meitz, R. Aucejo and E. Garcia-España, J. M. Llinares, C. Soriano and J. Alarcón, *Inorg. Chem.,* 2008, **47,** 6173; b) X. Zhao, Y. Liu, K. S. Schanze, *Chem. Commun.,* 2007, 2914; c) H. N. Lee, Z. Xu, S. K. Kim, K. M. K. Swamy, Y. Kim, S. J. Kim and J. Yoon, *J. Am. Chem. Soc.,* 2007, **129,** 3828; d) F. H. Huang, C. Cheng, G. Q. Feng, *J. Org. Chem.*, 2012, **77,** 11405.

10 a) M. J. Kim, K. M. K. Swamy, K. M. Lee, A. R. Jagdale, S. J. Kim, K. H. Yoon and J. Yoon, *Chem. Commun.,* 2009, 7215; b) X. Huang, Z. Guo, W. Zhu, Y. Xie and H. Tian, *Chem. Commun.,* 2009, 5143; c) Y. J. Jang, E. J. Jun, Y. J. Lee, Y. S. Kim, J. S. Kim and J. Yoon, *J. Org. Chem.,* 2005, **70,** 9603; d) L. Fabbrizzi, N. Marcotte, F. Stomeo and A. Taglietti, *Angew. Chem., Int. Ed.,* 2002, **41,** 3811.

11 a) S. Mizukami, T. Nagana, Y. Urano, A. Odani and K. Kikuchi, *J. Am. Chem. Soc.,* 2002, **124,** 3920; b) T. Y. Cheng, T. Wang, W. P. Zhu, X. L. Chen, Y. L. Yang, Y. F. Xu and X. H. Qian, *Org. Lett.,* 2011, **13,** 3656; (c) K. M. K. Swamy, S. K. Kwon, H. N. Lee, S. M. S. Kumar, J. S. Kim and J. Yoon, *Tetrhedron Lett.,* 2007, **48***,* 8683; d) N. Shao, J. Jin, G. Wang, Y. Zhang, R.Yang and J. Yuan, *Chem. Commun.,* 2008, 1127; e) C. M. G. dos Santos and T. Gunnlaugsson, *Dalton, Trans.,* 2009, 4712.

12 a) T. D. Rao, L. J. Liang and L. Y. Zhang, *Anal. Sci.,* 2013, 1165; b) H. Hofmeier, U. S. Schubert, *Chem. Soc. Rev.,* 2004, **33,** 373; c) J. L. Liang, X. J. Zhao and C. Z. Huang, *Analyst,* 2012, **137,** 953.

13 a) S. Bhowmik, B. N. Ghosh, V. Marjomäki and K. Rissanen, *J. Am. Chem. Soc.,* 2014, **136***,* 5543; b) T. Y. Cheng, T. Wang, W. P. Zhu, X. L.Chen, Y. J. Yang, Y. F. Xu and X. H. Qian, *Org. Lett.,* 2011, **13,** 3656.

14 a) R. M. Duke, E. B. Veale, F. M. Pfeffer, P. E. Kruger and T. Gunnlaugsson, *Chem. Soc. Rev.,* 2010, **39,** 3936; b) C. Lodeiro, J. L. Capelo, E. Oliveira, H. M. Santos, B. Pedras and C. Nunez, *Chem. Soc. Rev.,* 2010, **39,** 2948.

15 a) C. R. Lohani, J. M. Kim, S. Y. Chung, J. Y. Yoon and K. H. Lee, *Analyst,* 2010, **135,** 2079; b) A. R. Reddi, T. R. Guzman, R. M. Breece, D. L. Tiemey and B. R. Gibney, *J. Am. Chem. Soc.,* 2007, **129,** 12815.

View Article Online
DOI: 10.1039/C4DT03022B

Cd(II)-Terpyridine-based complex as a ratiometric fluorescent probe for pyrophosphate detection in solution and as an imaging agent in living cells

Shu-Yan Jiao, Kun Li*, Wei Zhang, Yan-Hong Liu, Zeng Huang, Xiao-Qi Yu*

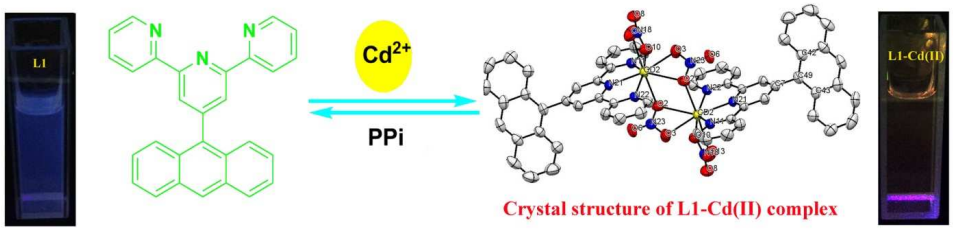

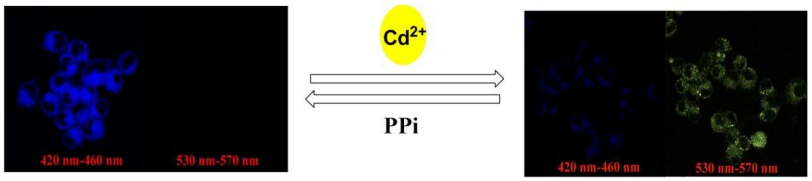

A ratiometric fluorescence probe for Cd^{2+} based terpyridine antracene ligand **L1** was synthesized and characterized. The results suggested that the probe could successfully applied in Cd^{2+} and pyrophosphate sensing in living cells.